Journal of Geoscience and Environment Protection, 2025, 13(4), 269-294
https://www.scirp.org/journal/gep
ISSN Online: 2327-4344
ISSN Print: 2327-4336

Application of Surface Complexation Model to ^{63}Ni Sorption to Selected Granitic Rocks and Minerals: Sorption at Varying pH

Fidelis Sameh Ebong[1,2*], Gillian Nkeudem Asoba[1], Frederick Ngolemasango Ediage[3,4], Nick Evans[2]

[1]Department of Social Economy and Family Management, Higher Technical Teachers' Training College, University of Buea, Kumba, Cameroon
[2]Department of Chemistry, Loughborough University, Loughborough, UK
[3]Research and Development Department, Fluorocarbon Ltd., Stevenage, UK
[4]Department of Chemistry, University of Buea, Buea, Cameroon
Email: *ebongf@yahoo.com

How to cite this paper: Ebong, F. S., Asoba, G. N., Ediage, F. N., & Evans, N. (2025). Application of Surface Complexation Model to ^{63}Ni Sorption to Selected Granitic Rocks and Minerals: Sorption at Varying pH. *Journal of Geoscience and Environment Protection, 13,* 269-294.
https://doi.org/10.4236/gep.2025.134015

Received: January 12, 2025
Accepted: April 15, 2025
Published: April 18, 2025

Abstract

The immobilisation of radionuclides in groundwater environments cannot be explained solely by the empirical models. These empirical models are not sensitive to the varying conditions that are found in nature. Sorption has been shown to be very sensitive to pH, Eh and ionic strength of the solution in which the radionuclides are found. Batch sorption experiments at different ionic strengths were conducted and LogK constants for the sorption processes were determined. JChess Geochemical code was used to compare experimentally and predicted Log K constants obtained from surface complexation reactions with different granitic rock samples. For pH dependent sorption, 1×10^{-5} mol·dm^{-3} solutions of $NiCl_2$ were prepared, and the pH was adjusted from 4 to 11, with intervals of 0.6 to 0.8 on the pH scale using NaOH (aq) and HCl (aq). Different concentrations of pH adjusting solutions were made from very weak to very strong acid or base. Sample separation was performed and counting was performed for Ni using the scintillation counter. Packard TRI-CARB 2750 TR/LL Liquid Scintillation Counter: Used for Ni sorption studies, counting from 0 to 67 keV to 2σ. Results showed varying sorption properties from one granitic mineral to the other. There was no effect of ionic strength on the sorption of Ni to Muscovite Mica (MM). Varying pH sorption isotherms for Ni sorption to Orthoclase Feldspar, showed experimental data and modelled matched for monodentate and bi dentate sorption using the same experimental conditions, modelling done assuming mono and bidentate complex formation. The following conclusions can be made after studying varying pH sorption

profiles of selected granitic rocks and mineral in different NaCl concentrations, using different models. Ni sorption is suppressed in the presence of NaCl, due to competition for the sorption sites.

Keywords

Surface Complexation, Sorption, Granitic Materials

1. Introduction

The immobilisation of radionuclides in groundwater environments cannot be explained solely by the empirical models discussed earlier. These empirical models are not sensitive to the varying conditions that are found in nature. Sorption has been shown to be very sensitive to pH, Eh and ionic strength of the solution in which the radionuclides are found. Using mass action laws, it is possible to describe sorption to heterogeneous samples such as granites by use of the surface complexation models. Surface complexation modelling approaches are generally more robust in their application over varying geochemical conditions than empirical models because they adopt a more mechanistic approach to sorption. This flexibility is often gained at the expense of simplicity, and SCMs may require a larger number of parameters to accommodate their increasing complexity. Surface complexation models use mass action laws analogous to aqueous phase reactions to describe adsorption thus, accounting for changes in chemical speciation, competitive adsorption, and other multi-solute interactive chemical effects. Atoms present in the bulk of the mineral are fully coordinated, whereas atoms at the surface are not, and so reactions with water give rise to hydroxylated surfaces. Outer sphere complexes are formed when a water molecule lies between the bound molecule or particles and the surface functional group, i.e., it is hydrated. Outer sphere complexation is usually rapid and reversible. Outer sphere complexes involve electrostatic interactions, whereas inner sphere interactions form from chemical bonds. Therefore, there is a chemical difference between an ion bound in the inner sphere and an ion of the same species bound in the outer sphere or present in the diffusion part of a double layer (Allison, 2004).

Inner sphere complexes are formed when a water molecule or particle is bound to the functional group. As a rule, the relative affinity of a contaminant to sorb will increase with its tendency to form inner sphere surface complexes (Hayes & Katz, 1996). The tendency for a cation to form an inner-sphere complex in turn increases with increasing valency. Inner sphere complex formation is usually slower than outer sphere complexes and often irreversible, and can increase, decrease, neutralise, or reverse the charge on the particle regardless of the original charge. Adsorption of ions via inner sphere complexation can occur on the surface regardless of the surface charge. It should be noted that inner and outer sphere complexation can occur at the same time (Sparks, 2002).

1.1. Application of Mass Law to Surface Complexation of Radionuclides

The general equation for the interaction of the metal ion with an oxide substrate may be expressed by the following equation (Kanungo, 1994; Tripathy et al., 2006).

$$M^{n+} + x(\equiv SOH) = \left[M(\equiv SOH)_x\right]^{(n-x)+} + xH^+ \quad (1)$$

The equation above is applicable under the following assumptions:

- Protons are the dominant potential determining ions.
- All surfaces have at least single binding site.
- Each site can undergo two protonation reactions.
- Charges are always expressed as integers.
- Strict distinction is maintained between inner- and outer-sphere complexes.

For very low activities of metal species and those of its complexes with surface species, the equilibrium constant may be expressed as (Kanungo, 1994; Tripathy et al., 2006).

$$\mathrm{Log}\left[\frac{M^{n+}_{absorbed}}{M^{n+}_{aoln}}\right] = \log K_e + x\left(pH + \log[\equiv SOH]\right) \quad (2)$$

The equilibrium constant K_e describes the distribution of a given constituent among its possible chemical forms if complex formation and dissociation reactions are at equilibrium. The equilibrium constant is affected by several factors, including the ionic strength of the aqueous phase, presence of competing reactions, and temperature (Hayes & Katz, 1996). A plot of the left-hand side as a function of {pH + log [≡SOH]} yields a linear relationship, the slope of which gives the stoichiometry of the reaction. This relationship is applicable in the region of steep rise in adsorption with pH (Kanungo, 1994). Values of "x" (x is a dimensionless constant) greater than unity suggest a mixed reaction type. If the adsorption is smeared, the proton stoichiometry in the region of lower pH value is even lower than 0.05 an indication that adsorption takes place in the β-plane (Kanungo, 1994).

1.2. Basics of Surface Complexation Modelling

In the surface complexation model, which is applied primarily to oxides and silicate minerals, mineral surfaces are characterised as polymeric oxo acids, the specific adsorption of protons or hydroxide ions is interpreted in terms of acid-base reactions at the surface. Surface charge is developed by reactions yielding charged surface species (e.g. protonated or deprotonated surface hydroxyl groups) (Hering and Kraemer 1994). This serves as the basis for the application of the electric double layer model of surface complexation. A general term (hydr)oxide is used to describe all potential sorbents occurring as oxides, hydroxides and oxyhydroxides (Lützenkirchen & Behra, 1996). In modelling sorption of radionuclides to surfaces at varying pH, the surfaces of the mineral are considered too complex to be quantified in terms of the contributions of individual phases to adsorption. Instead, it is assumed that adsorption can be described by SCM equilibria written for "ge-

neric" surface functional groups, with the stoichiometry and formation constants for each SCM mass law evaluated based on simplicity and goodness-of-fit (Goldberg et al., 2007). The generic surface sites represent average properties of the granite type rather than specific minerals.

1.3. Main Assumptions of SCM

This model is predictive and extending it to natural samples involves certain assumptions such as:

- Sorption occurs through interaction with the hydroxyl groups.
- Constituent minerals are uncoated and do not interact with each other.

This model has been applied in calculating the proton stoichiometry (PS) at the point of steep rise in sorption with pH (Kanungo, 1994). This plot defines the narrowest region in the adsorption spectrum of a pH range and gives the Log K_e (equilibrium constants) values. Because R_d values are very sensitive to pH, as we shall see in the sections that follow, the R_d concept will have limited application in describing sorption processes that take place over a range of pHs. However, an indication of the R_d will be shown on plots of against pH for ease of comparison. The general equations for the interaction of the metal ion with oxide substrate may be expressed by Equation (1) and Equation (2).

1.4. Objectives

The aim of this work was to study ^{63}Ni sorption properties on some granitic rocks and minerals. The objective was to investigate radionuclide immobilisation in the far-field of a radioactive waste repository, using primarily batch sorption techniques. In this context, attention was paid to granitic rock as a potential repository host rock. Ionic strength is an important factor controlling the behaviour of metal cations, such as their hydrolysis, and the distribution coefficients for their adsorption on mineral surfaces (Yoshida & Suzuki, 2006). Most field and laboratory experiments are conducted at low ionic strengths. However, only limited knowledge exists on the effects of ionic strength on the migration of cations in porous media (Yoshida & Suzuki, 2006). Apart from ionic strength, the ability of geologic materials to exhibit high sorption at low pH values will depend very much on the position of the point of zero charge (pH at which the net surface charge is zero) for the surfaces. Geologic materials such as granite and its minerals exhibit relatively low points of zero charge (USEPA, 1999). This work investigates the effect of pH on sorption at constant metal concentration, using ^{63}Ni. Different granitic rocks and granitic minerals have been used in the sorption experiments to understand the sorption profile, and the sorption edge (pH at which there is a sharp rise in sorption with pH). Sorption parameters to quantify the sorption processes have been calculated, from the sorption data. Surface complexation modelling using the JChess geochemical code, has been performed.

^{63}Nickel

Research on radionuclide migration and adsorption has centred on radionuclides of elements such as uranium, plutonium, caesium, and strontium (Everett,

1998; Ohnuki, 1994; Vandergraaf et al., 1997; Rumynin et al., 2005; Bernard, 1995). Ni sorption to granites has not been researched to the same extent (Ticknor, 1994; McKinley & Hadermann, 1984; Higgo, 2007; Andersson, 1988). The isotope ^{63}Ni is an artificial radionuclide. The presence of ^{63}Ni in the environment results mainly from activities such as; nuclear weapon tests, radioactive effluents from nuclear installations and accidental releases from nuclear power plants (e.g. Chernobyl) (Scheuerer et al., 1995). ^{63}Ni is formed by neutron capture of stable ^{62}Ni. ^{63}Ni is a β-emitter with a half-life of 100.1 years (Knol et al., 2008). Naturally occurring nickel is composed of 5 stable isotopes; ^{58}Ni, 60Ni, ^{61}Ni, ^{62}Ni and ^{64}Ni, with ^{58}Ni being the most abundant (68.077% natural abundance). 18 radioisotopes have been characterised with the most stable being ^{59}Ni with a half-life of 76,000 years (decay mode is by electron capture to ^{59}Co and decay energy of 1072 MeV), ^{63}Ni with a half-life of 100.1 years, and ^{56}Ni with a half-life of 6.077 days. All the remaining radioactive isotopes have half-lives that are less than 60 hours and the majority of these have half-lives that are less than 30 seconds. ^{63}Ni is a beta-emitting radionuclide of E_{max} = 67 keV. It exists in the coolant water of nuclear power reactors and is formed by neutron capture of nickel released from steel piping and so on due to corrosion.

^{62}Ni + 1n → ^{63}Ni neutron capture process (6.80 MeV) (Treado & Changnon, 1961)

^{63}Ni → ^{63}Cu decay energy = 0.067 MeV.

The Different energies and decay pathways are shown in **Table 1**.

It is included in the list of low-level long-lived radioactive waste from nuclear power reactors (L'Annunziata, 2004). Nickel can be transported as particles released into the atmosphere or as dissolved compounds in natural waters (Australian Government, 2023).

Table 1. Radioactive properties of key Ni isotopes, showing the different decay modes and energies (Argonne National Laboratory EVS, 2005).

Isotope	Half-Life (yr.)	Decay Mode	Radiation Energy (eV)		
			Alpha (α)	Beta (β)	Gamma (γ)
^{59}Ni	75,000	EC	-	4600	
^{63}Ni	100	β	-	17,000	-

EC = electron capture, GBq = Giga Becquerel, g = gram, and eV = electron volts; a dash means the entry is not applicable.

Values from Argonne National Laboratory, Human health fact sheet of 2005 (Argonne National Laboratory EVS, 2005).

1.5. Granite as a Suitable Host Rock for a Deep Repository

Geological matrices surrounding a waste repository are expected to act as natural barriers to both water flow and radionuclide migration. Granite rock as host media and bentonite, alone or its mixture with sand (quartz) or crushed granite, as the backfill are the favoured materials in the Swedish model for the repository

(Allard et al., 1980). Granite, the most common igneous rock is the candidate for a repository host rock in Sweden and Finland (Guillaumont, 1994; Baston et al., 1994). Physical properties lending uniqueness to granite are its porosity/permeability and hardness. Granite has almost negligible porosity coupled with a high thermal stability. Granite is virtually impervious to weathering by temperature, and even from chemicals, and has a very small coefficient of expansion. Many studies on granite reveal the main composition to be quartz, plagioclase feldspars and biotite (Papelis, 2001; Sarah, 1994; Höolttä et al., 1998; USEPA, 1999). Hydraulic properties of granitic rocks which may be used as part of the Geologic Barrier System (GBS) include; gently dipping zones, transmissive, upper part of granitic rock mass can highly transmissive, greater than 200 m depth low frequency of connected transmissive fractures, greater than 400 m depth very few connected transmissive fractures, meteoric water at shallow depth, below which salinity increases (Andersson, 2008). Granites from different sources vary in mineralogical composition, which can result in differences in sorption properties in different types of granite.

2. Experimental: pH Dependent Sorption of ^{63}Ni at Constant Metal Concentration

To investigate the effect of ionic strength as well as pH, two sets of experiments, in the presence of 0.1 and 0.05 mol·dm^{-3} NaCl, were used with a control having no NaCl present. The effect of surface area has been taken into consideration in the surface complexation studies using the JChess geochemical code. This chapter reports a study of the effect of pH on sorption of radionuclides to some granitic rocks and minerals. NaCl is used to create a low concentration brine/seawater environment. With the possible disposal/storage of nuclear waste in deep geological repository, and with the potential rise in sea levels due to climate change, there is growing concern regarding the possible intrusion of brine into repository vaults. Thus, it is important to understand the effect of sea water on sorption of radionuclides in the far-field.

For pH dependent sorption, 1×10^{-5} mol·dm^{-3} solutions of $NiCl_2$ were prepared, and the pH was adjusted from 4 to 11, with intervals of 0.6 to 0.8 on the pH scale using $NaOH_{(aq)}$ and $HCl_{(aq)}$. Different concentrations of pH adjusting solutions were made from very weak to very strong acid or base. This was important, to be able to vary the pH without significantly altering the concentration of the Ni solution. To move the pH to a lower pH value of about 4, a strong acid was preferred since very little volume of the acid was required thus, minimising the impact on the overall concentration of the solution. 0.1 g of every sample were weighed into a 20 cm^3 vial and 20 cm^3 of pH-adjusted solutions were added. 0.1 cm^3 of spike solution was added. After shaking the batch was allowed to equilibrate over a period of 5 to 7 days. The effect of ionic strength was investigated by the addition of different amounts of NaCl in the bulk $NiCl_2$ solutions to give ionic strengths of 0.05 and 0.1 mol·dm^{-3} NaCl solutions. Sample separation was

performed as described above and counting was performed for Ni using the scintillation counter. Packard TRI-CARB 2750 TR/LL Liquid Scintillation Counter: Used for Ni sorption studies, counting from 0 to 67 keV to 2σ (i.e. 95% of the counts fall within the confidence interval) for 20 min, and for measurements of calibration standards for the work on autoradiography. One powerful technique in radionuclide detection is Liquid Scintillation Counting (LSC). Although the technique is sensitive to alpha and, to a lesser extent, gamma emitting radionuclides, LSC is most extensively used for the determination of beta-emitters. The main advantage of LSC as compared to solid state detectors is its high-detection efficiency, and ability to detect low-energy beta emitters. However, as with any spectrometric technique used for beta assay, only limited spectral information is obtained as beta energy spectra are continuous from zero to the maximum energy value (Mellado et al., 2005).

3. Results and Discussion

Sorption reactions at solid-water interfaces decrease solute mobility and often control the fate, bioavailability, and transport of radionuclides. Adsorption of metals in solution generally become more specific as the pH increases, i.e. formation of inner sphere complexes is favoured at elevated pH. Based on sorption experiments, the pH dependent sorption on mineral surfaces is usually modelled assuming two types of sites (Scheidegger et al., 1996):

- Ion exchange, or nonspecific adsorption, sites that exchange background electrolyte cations with weakly bound hydrated metal ions (outer sphere complexes).
- Specific adsorption at amphoteric surface hydroxyl sites such (Al-OH, Si-OH) in which the surface sites hydrolyse and then bond directly to surface O or OH groups and are not easily displaced by electrolyte (inner sphere complexes) (Scheidegger et al., 1996). This usually occurs at low sorbate concentrations. With increasing pH or sorbate concentrations, precipitation can occur. When a precipitate contains chemical species derived from both the solution and the dissolution of the sorbent mineral, it is referred to as a coprecipitate (Dähn et al., 2003).

3.1. Ni Sorption to Granitic Rocks

Three sets of experiments were performed, to study the influence of pH and ionic strength on Graphic Granite (GG), Granite Adamellite (GA) and Rapakivi Granite (RG). Results have been plotted as sorption isotherms at varying pH, following experimental protocol described in section 2. As the isotherms showed a similar pattern for the different granitic rocks considered, GG is presented.

Using Ni speciation results for the three systems studied (**Figures 1(A)-(C)**) above pH 8.5 precipitation of Ni occurred. However, immobilisation mechanisms can include precipitation of the metal on solid surfaces (Jedináková-Křižová, 1998). Thus, precipitation occurring at high pH values in the present of solid is considered as immobilisation in this work. Deductions from experimental results

for Ni sorption to GG thus, include:

1) pH had no significant effect in the NaCl free solution below pH 8.5 and above pH 8.5.

2) Sorption varied with pH and equilibrium state is attained after pH 8 for sorption in 0.05 mol·dm^{-3} NaCl.

3) Sorption in 0.1 mol dm^{-3} NaCl showed the same sorption profile as that in 0.05 mol·dm^{-3} NaCl. This is evident from the JChess speciation diagrams (Figure 1 and Figure 2). Speciation of Ni in the two NaCl systems studied did not vary, with Ni^{2+} as the main species.

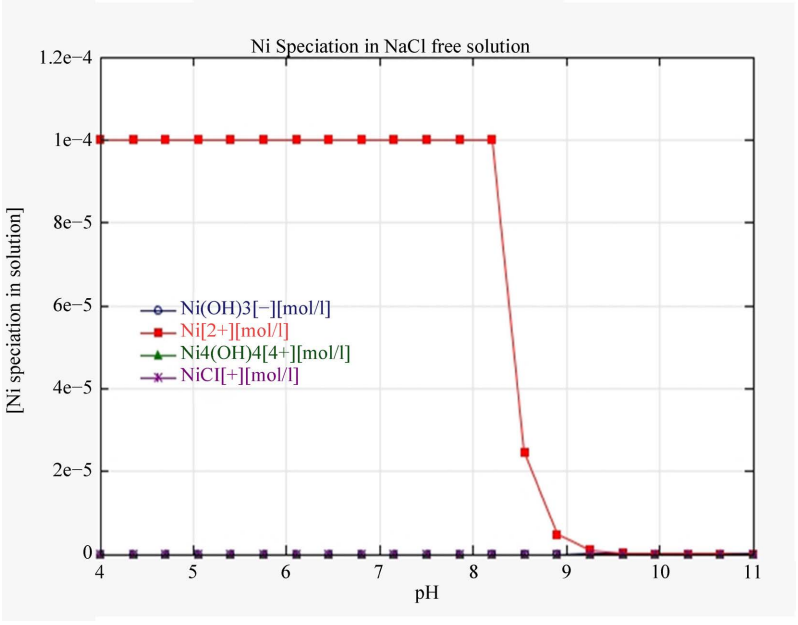

(a)

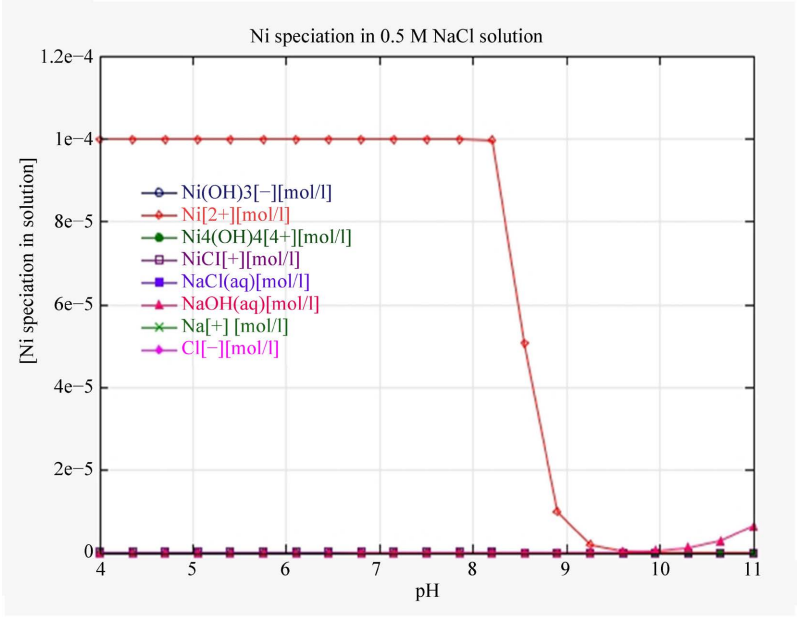

(b)

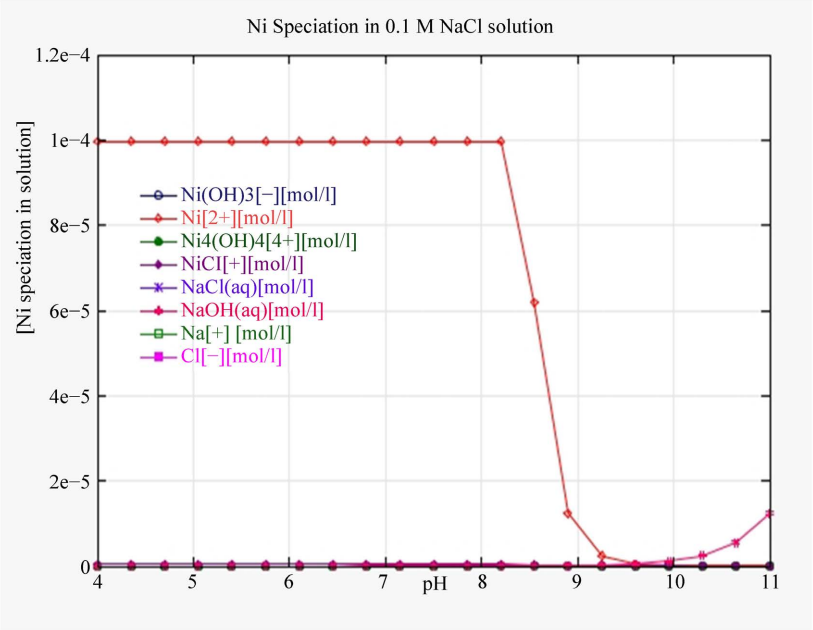

(c)

Figure 1. A, B and C: Ni^{2+} aqueous speciation, showing the variation of Ni metal concentration with pH in different NaCl systems. The expanded Y-axis for the speciation above pH 8 is shown in the figure below, with the major species being, $Ni(OH)_2$ and $Ni(OH)^{3-}$ (van der Lee, 2003).

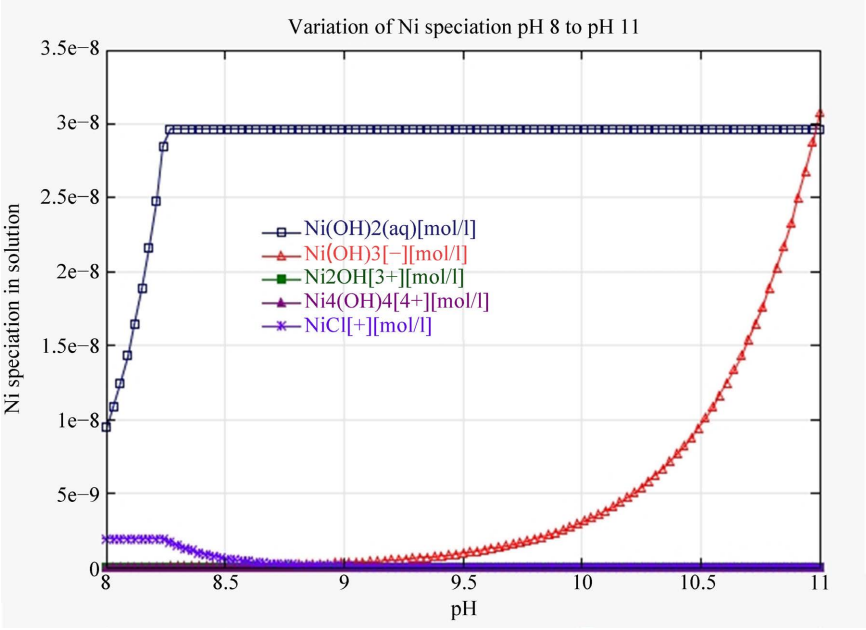

Figure 2. Expanded Y-axis showing Ni aqueous speciation in the pH range 8 - 11, showing the major species $Ni(OH)_2$ and $Ni(OH)_3^-$ probably responsible for Ni sorption within the pH range 8 to 11 (van der Lee, 2003).

Granitic rocks are composed of silanol and aluminol sites with a PZC between 4 and 5 (Sposito, 1984). Thus, the mineral surfaces will be negatively charged

across the pH range studied. However, sorption showed pH dependency in 0.05 and 0.1 mol·dm^{-3} NaCl solutions. However, in the pH region 4 to 6, there was no steep rise in sorption with pH for GG, GA, or RG. The absence of a steep increase in sorption in the pH range 4 to 6 is often interpreted as being due to cation exchange on the permanently charged planar sites (Bradbury & Baeyens, 2009).

Sorption in 0.05 and 0.1 mol·dm^{-3} NaCl systems was affected by the presence of Na^+ ions competing for the sorption sites. This is obvious based on the fact sorption in the absence of Na^+ ions; sorption was independent of pH within the entire pH range studied. Thus, despite the large charge to volume ratio of Ni, sorption is suppressed in the presence of Na^+ ions below pH 7 for sorption in NaCl systems. However, above pH 8, no difference in the sorption profiles of the three systems is observed. Traditionally, ionic strength dependent sorption is used to distinguish between specific and non-specific sorption. Outer sphere complexes involve only weak electrostatic interactions and are strongly affected by the ionic strength of the aqueous phase, whilst inner sphere complexes involve much stronger covalent or ionic binding and are only weakly affected by the ionic strengths (Scheidegger et al., 1996). From **Figures 3-5**, the sorption process is affected by ionic strength. For solutions containing NaCl, sorption can be said to be inner-sphere at pH > 7. At pH > 7, there is a significant rise in sorption and sorption is not affected by pH. As seen in section 1.1, the mass action law can be applied to the surface complexation process with the stated assumptions. Thus, plotting Log Rd as a function of {pH + Log [≡SOH]} yields a linear relationship, the slope of which gives the proton stoichiometry of the reaction and the intercept defines the equilibrium constant, as shown in the figure below.

Plotting Log R_d as a function of {pH + Log [≡SOH]} assumes that the activity (concentration) of the sorption sites is 1 (Hayes & Katz, 1996). From **Figure 4** and **Figure 5** the region of significant (steep) rise in sorption (the sorption edge) is defined between pH 7 to 8. From the gradient of the plot, the Proton Stoichiometry (PS) is determined (Hayes & Katz, 1996). Thus, from **Figure 4**, and **Figure 5**, the proton stoichiometry is 1.9 and the sorption edge is between 7 and 8. When sorption is not affected by variation in pH, the model used above (the Kurbatov model) is not applicable, since there is no region of significant rise in sorption with pH, under the stated experimental conditions.

The relationship (Equation (1)) is applicable in the region of steep rise in adsorption with pH (Kanungo, 1994). Values of "x" greater than unity suggest a mixed reaction type. Analysing the results based on the above model yielded proton stoichiometry values for Ni sorption to granitic rocks.

From the results shown in **Table 2** some conclusions can be reached.

1) There is no region of steep rise in sorption, for NaCl free solution for all granitic rocks studied;

2) Sorption to Biotite Granite (BG) and Grey Granite did not vary with pH for all three systems studied since there is no region of steep rise in sorption with pH;

3) The concentration of Na^+ ions affected the sorption of Ni^{2+} in 0.05 and 0.1 mol dm^3 NaCl solutions below the sorption edge.

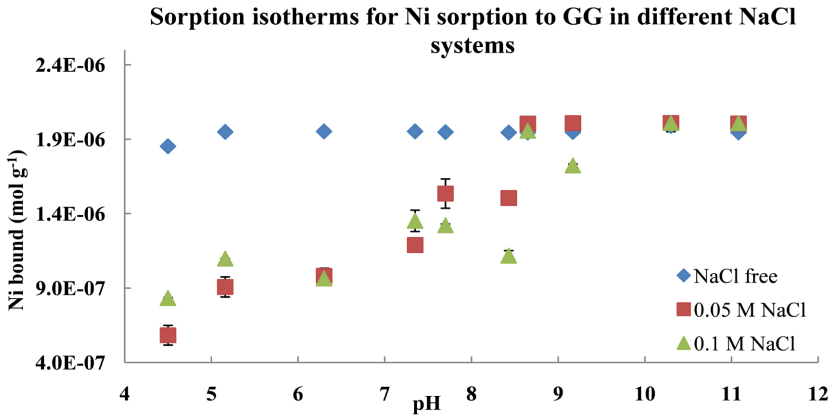

Figure 3. Effect of varying pH on the sorption of Ni to Graphic Granite at constant metal concentration of Ni. Figure showing sorption profile of Ni in different ionic strength environments, equilibrating ca. 8 days with liquid solid ratio of 200:1, at rtp.

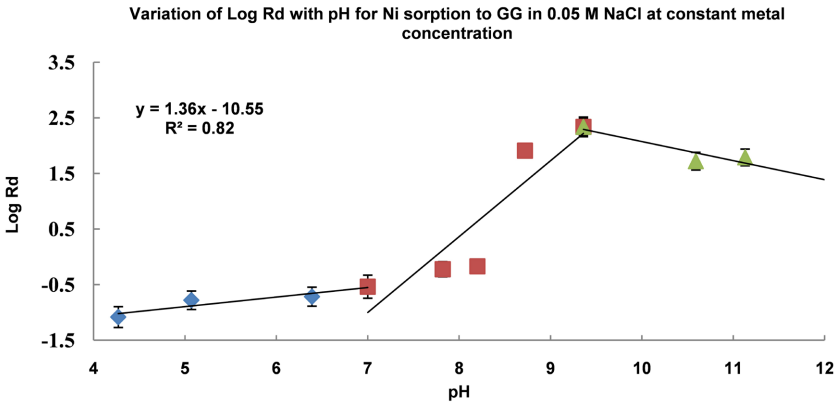

Figure 4. Log Rd as a function of pH for Ni sorption to Graphic Granite at constant metal concentration in 0.05 mol·dm^{-3} NaCl solution. Figure shows region of steep rise in sorption within a narrow pH range (sorption edge), and region of gentle increase in sorption with pH. Equilibrating ca. 8 days with liquid solid ratio of 200:1, at rtp.

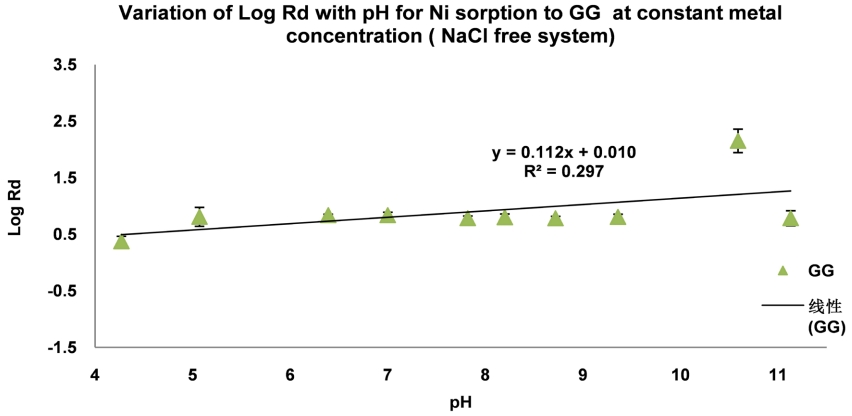

Figure 5. Log R_d against pH for Ni sorption to Biotite Granite, and Grey Granite at constant metal concentration in 0.1 mol·dm^{-3} NaCl solution. Figure shows no region of steep rise in sorption (sorption edge), and no region of gentle increase in sorption with pH. Equilibration time: ca. 8 days with liquid solid ratio of 200:1, at rtp.

Table 2. Ni sorption to granitic rocks at constant metal concentration and the application of the mass action law. Log Ke values are derived from the slope, at the region of steep rise in sorption with pH. Model did not apply to BF and GG.

	pH dependent Sorption.								
	I = 0.1 (mol·dm^{-3})			I = 0.05 (mol·dm^{-3})			NaCl free		
	SE pH	PS	Log K_e	SE pH	PS	Log K_e	SE pH	PS	Log K_e
GG	7 - 8.5	1.13	−13.71	7.5 - 9	1.4	−10.6	No fit		
GA	7 - 9.5	0.75	−5.72	7.85	1.2	−10.6	No fit		
RG	7.5 - 8	0.73	−5.70	7 - 8.2	1.1	−6.9	No fit		

SE pH = sorption edge pH; PS = proton stoichiometry; K_e = the equilibrium constant for the reactions that lead to the protonation/deprotonation reaction as applied in the electric double layer model.

Understanding the sorption behaviour and properties of granitic rocks is complex. Sorption of metallic ions on to granitic surfaces will depend on the mineralogical composition of the granitic rock; rocks with high quartz content will be low sorbing, based on the low sorption capacity of quartz as seen by Ticknor (Ticknor, 1994). The complexity of the sorption process to heterogeneous materials such as granite will depend amongst other parameters on the net surface charge, which in itself depends on the point of zero charge of the individual minerals of the bulk sample, and the structure of the granitic sample in general. This will affect the diffusion of particles (non-electrostatic sorption) into the microstructure, as such affecting the net retention property of the granitic rock. Due to the lack of literature data on work relating to the sorption of Ni to bulk samples such as granitic rocks across the pH range, it has not been possible to compare the results obtained. However, sorption data obtained for the rest of the experiments in this work has been treated following the same approach, but in some only the sorption parameters are shown.

3.2. Ni Sorption to Granitic Minerals

Quartz, feldspar, and mica are the major constituent minerals of most granitic rocks (**Table 3**). However, due to their structural and chemical differences, radionuclide retardation on the surfaces of these minerals might vary. As shown in previous work by Ebong and Nick (Ebong & Nick, 2012; Ebong & Nick, 2011; Ebong & Nick, 2008) quartz is low sorbing compared to mica at constant pH. As the pH of the solution changes, the potential for OH groups on the mineral surfaces to be protonated or deprotonated changes. This process of protonation/deprotonation depends on the point of zero charge of the mineral. Quartz constitutes about 25 to 50% by weight composition depending on the granite type (Allard et al., 1980; Muuronen et al., 1985). SiO_2 is the main constituent of quartz. Quartz has been reported to sorb radionuclides very weakly compared to other minerals such as feldspars and biotite (Anderson et al., 2007). Biotite has one of the four silicon atoms substituted by an aluminium atom, creating a negative

charge which is balanced by potassium cations which hold adjacent layers together (Cresser et al., 1993). Feldspars are anhydrous three-dimensional aluminosilicates of linked SiO_4 and AlO_4 tetrahedra that contain cavities that can hold mono and divalent cations to maintain electrical neutrality (Sparks, 2002). They can be divided into two main groups; alkali feldspars ranging from K aluminosilicates (Orthoclase Feldspars) and Na to Ca aluminosilicates (Plagioclase Feldspars).

Table 3. Chemical composition of different minerals found in granite, adapted from (Allard et al., 1980).

Mineral	Chemical composition
Quartz	SiO_2
Muscovite	$K(Mg,Fe)_3(AlSi_3O_{10})(OH)_2$
Orthoclase Feldspar	$KAlSi_3O_8$
Plagioclase Feldspar	$NaAlSi_3O_8/CaAl_2Si_2O_8$

3.3. Results from Sorption Experiments and Modelling with JChess Geochemical Code

In the surface complexation model, the surface sites are treated as amphoteric groups. Protonation or deprotonation reactions occur on the surface groups resulting in charged surfaces onto which metal ions bind. Consider the sorption of Ni to a mineral with surface ≡SOH, the following are possible:

$$\equiv \mathrm{SOH} \rightleftharpoons \mathrm{SO}^- + \mathrm{H}^+ \rightarrow \text{deprotonation}$$

$$\equiv \mathrm{SOH} + \mathrm{H}^+ \rightleftharpoons \mathrm{SOH}_2^+ \rightarrow \text{protonation}$$

Surface complexation equation for the deprotonation reaction will be written as:

$$\equiv \mathrm{SOH} + \mathrm{Ni}^{2+} \rightleftharpoons \equiv \mathrm{SONi}^+ + \mathrm{H}^+$$

The equilibrium constant for the reaction can thus, be written as

$$K = \left[\equiv \mathrm{SONi}^+\right]\left[\mathrm{H}^+\right] / \left[\equiv \mathrm{SOH}\right]\left[\mathrm{Ni}^{2+}\right]$$

The equilibrium constant defined above is thus, corrected for electrostatic interactions to obtain the intrinsic equilibrium constant as shown below (Guo et al., 2010).

$$K_S = \frac{\left[\equiv \mathrm{SONi}^+\right]}{\left[\equiv \mathrm{SON}\right]} - \frac{\left[\mathrm{H}^+\right]}{\left[\mathrm{Ni}^{2+}\right]} \frac{\left[\gamma_{\mathrm{H}}^+\right]}{\left[\gamma_{\mathrm{Ni}}^{2+}\right]} e^{(F\varphi/RT)}$$

where S is the surface, F is the Faraday constant (magnitude of electric charge per mol of electron $C \cdot mol^{-1}$), ψ is the surface potential (V), R is the real gas constant ($J \cdot K^{-1} \cdot mol^{-1}$), and T is the temperature (K), γNi^{2+} and γH^+ are the activity coefficients of Ni and H^+ respectively. Most methods by which the intrinsic equilibrium constant for the surface complexation of metal ions to mineral surfaces is determined involves, the application of geochemical codes such as PHREEQC, MINTEQA2 and JChess (Guo et al., 2010, Bradbury & Baeyens, 2009; van der Lee, 2003). In this work

JChess geochemical code by Ecole de Mines de Paris France (van der Lee, 2003) provided by Loughborough University has been used. Results from sorption experiments are presented in the following sections. Experimental results are accompanied in some cases by surface complexation based predictive models.

3.4. Ni Sorption to Quartz

Rose Quartz (RQ) as in Figure 6, Figure 7 and Figure 7 was chosen as a representative sample of quartz. Ni sorption to RQ showed that below pH 8, sorption was low (mean R_d values below pH of 8 were < 5 $cm^3 \cdot g^{-1}$, while above pH > 8 the mean R_d was 1.7 $cm^3 \cdot g^{-1}$) and not affected by pH Na^+ ions did not affect the sorption capacity below pH of 8. The observed low sorption capacity can be due to ions bind. A steep rise in sorption is observed above pH of 8. Sorption parameters are shown in Table 4. Proton stoichiometry (proton stoichiometry is the number of protons released or adsorbed the surface sites to form $\equiv SO^-$ or $\equiv SOH^{2+}$) values close to 2 are calculated for MM and RQ, for sorption in 0.1 $mol \cdot dm^{-3}$ NaCl solution.

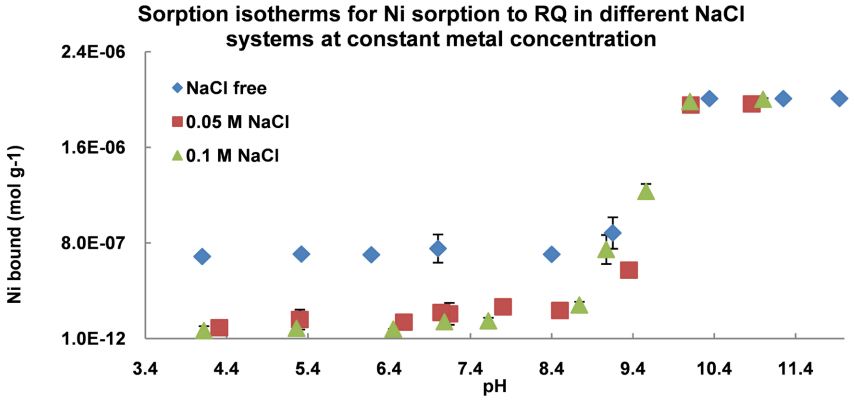

Figure 6. Varying pH sorption of Ni to Rose Quartz at constant metal concentration of Ni. Figure showing sorption profile of Ni in different ionic strength environments, equilibrating ca. 8 days with liquid solid ratio of 200:1, at rtp. Two sorption regions are shown relating sorption by CE and by SC.

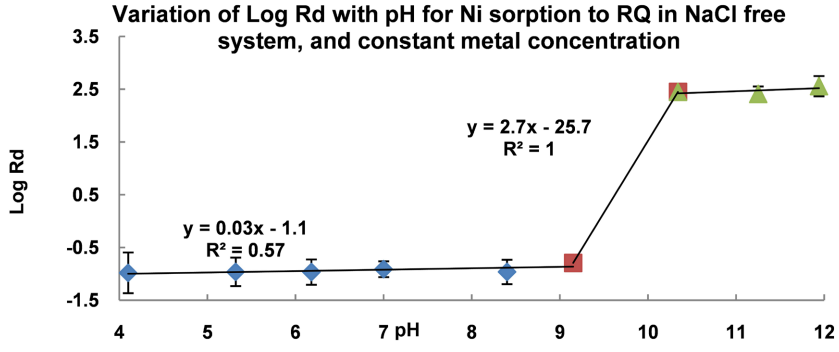

Figure 7. Log R_d as a function of pH for Ni sorption to Rose Quartz at constant metal concentration in NaCl free solution. Figure shows region of steep rise in sorption within a narrow pH range (sorption edge), and region of gentle increase in sorption with pH equilibrating ca. 8 days with liquid solid ratio of 200:1, at rtp.

Table 4. Varying pH sorption of Ni to granitic minerals at constant metal concentration. Table shows the proton stoichiometry at the stated sorption edges, obtained from the gradient in region of significant rise in sorption with pH. Values derived from plots like that shown in Figure 11. The model is not applicable to BM and MM due to the absence of region of steep rise in sorption.

Varying pH sorption of Ni to granitic minerals									
Sample	I = 0.1 (mol·dm^{-3})			I = 0.05 (mol·dm^{-3})			NaCl free (mol·dm^{-3})		
	SE pH	PS	Log K_e	SE pH	PS	Log K_e	SE pH	PS	Log K_e
RQ	8.5 - 10	1.9	−15.4	8.5 - 9.5	2.6	−22.6	8.5 - 9.5	2.7	−25.7
MQ	8.5 - 10	1.9	−15.2	8.5 - 10	2.6	−22.48	8.5 - 10	1.66	−22.01
OF	7 - 9.5	0.5	−4.9	7.5 - 10	0.65	−2.72	8.5 - 11	0.43	−1.23
PF	8.5 - 9.5	0.7	−3.2	8.5 - 9.5	1.03	−6.65	9.5 - 11	0.69	−3.49

3.5. Results from Surface Complexation Modelling-Quartz

Titrimetric experiments were conducted to determine the proton exchange capacity for different minerals. measured equivalence points from titrimetric measurements with NaOH. The surface charge was calculated, using BET surface area measurements. Surface complexation input parameters, such as; proton exchange capacity, particle radius, temperature, equilibration time and pH were used in the surface complexation modelling. Using the data obtained from the JChess code, to plot sorption isotherms required corrections to be made to the output data. The output data are given in mol·dm^{-3} (fixed concentration). However, the data were converted to mol·g^{-1} as used in plotting the sorption isotherms in the sections that follow. In using the surface complexation model, the denticity of the process is used. Denticity is defined here as the number of Ni ions that are bonded to the surface site. As such, mono and bidentate bonding refers to Ni atoms bonded to one of more surface sites. Figure 8 is the varying pH sorption isotherms for Ni sorption to Rose Quartz, showing data obtained from experiment and modelling, using JChess using Log K = −7 for mono and bidentate binding. Output parameters were collected and are stated in Table 5.

Surface complexation modelling in NaCl free system, 0.05 mol·dm^{-3} NaCl system, and 0.1 mol·dm^{-3} NaCl system were carried out. Figure 9 shows predicted and experimental fits for the SCM in NaCl free system. Comparing the modelled and experimental isotherms (Figure 8), both sets of data showed similarities within the limits of error as stated below:

Sorption did not vary with pH for both modelled and experimental data, below pH 8:

- Sorption capacity was low below pH 8 for both sets of data.
- The sorption edge (region of significant rise in sorption within a narrow pH change) determined from the Kurbatov model (Log Rd against pH plots are referred to as Kurbatov plots derived from the Kurbatov model. From Figure 8 sorption showed a significant increase within pH range of 7.5 and 8.5. This narrow pH is called the sorption edge pH. Sorption parameters are shown in Table 4 for Ni sorption to granitic minerals.

Table 5. Concentration of site occupancy for Ni sorption to quartz in different NaCl environments. Log K value of −7 for mono and bidentate systems. Exchange capacity 5×10^{-2} μmol·m^{-2} calculated from titrimetric experiments with 0.1 g of Rose Quartz (particle size of 46 - 250 microns). Figures in table relate to the concentration of metal-solid binding sites in the system as calculated by the JChess output. Values show that sorption is overwhelmingly monodentate.

Site	NaCl free (mol·dm^{-3})	0.05 mol·dm^{-3} NaCl (mol·dm^{-3})	0.1 mol·dm^{-3} NaCl (mol·dm^{-3})
≡Quartz-O-Na	-	7.9×10^{-9}	1.4×10^{-11}
≡Quartz-O-Ni^{+}	1.8×10^{-11}	1.5×10^{-12}	3.8×10^{-12}
(≡Quartz-O)$_2$Ni	4.9×10^{-22}	3.6×10^{-23}	1.0×10^{-18}

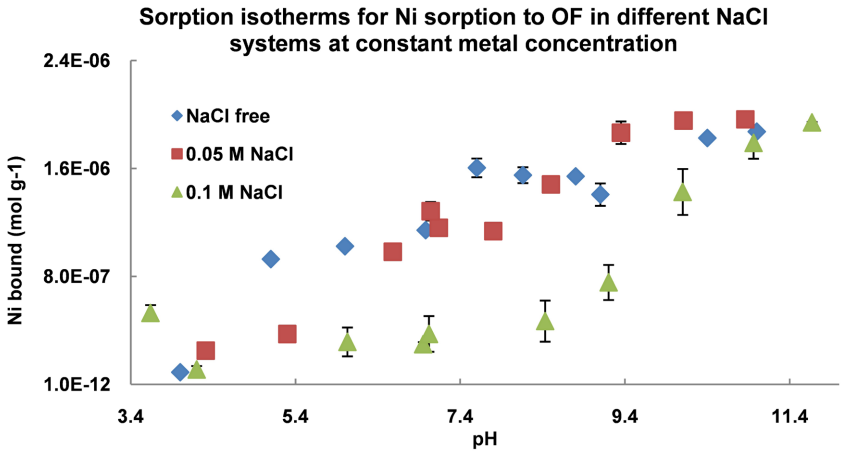

Figure 8. Varying pH sorption of Ni to Orthoclase Feldspar in different concentrations of NaCl, at constant metal concentration of Ni, equilibration ca. 8 days with liquid solid ratio of 200:1, at rtp.

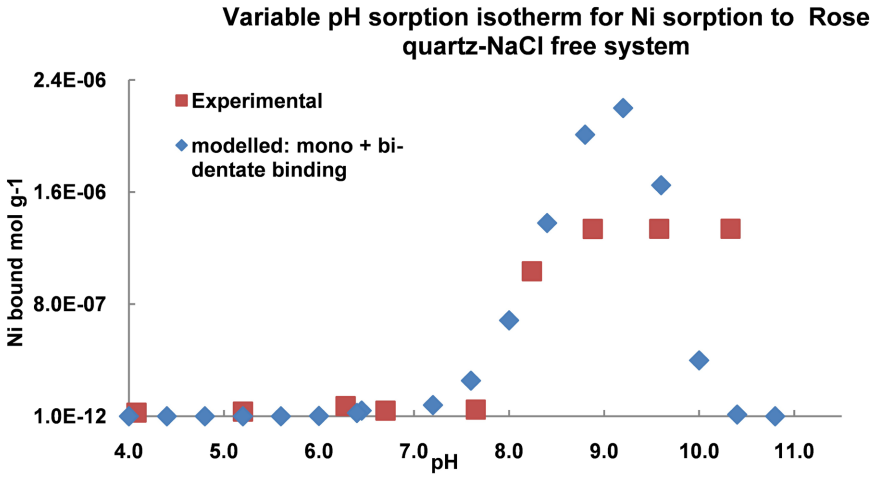

Figure 9. Varying pH sorption isotherms for Ni sorption to Quartz. Figure showing data from experimental data and data obtained from JChess Code, using the same experimental conditions, modelling done assuming mono and bidentate complex formation. Equilibrating ca. 8 days with liquid solid ratio of 200:1, at rtp.

Despite the similarities in the experimental and theoretical model, two major differences are apparent:

1) The models differed in the maximum amount of Ni bound. From the isotherms, the maximum amounts of Ni bound at the region of steep rise in sorption are 1.3×10^{-6} and 2.2×10^{-6} mol·g^{-1} for experimental and theoretical models respectively.

2) The JChess model showed that sorption decreases to zero at pH 11, whereas for the experimental data, sorption showed saturation.

The reason for the difference between the two models can be due to the purity of the mineral. Quartz (Rose Quartz) found in environmental samples can contain impurities such as titanium, iron and manganese, in the crystal structure (mindat.org 2012). These impurities can affect the overall sorption capacity of the mineral. Another reason can be due to sorption due to non-electrostatic forces (as in SC models); impurities in the crystal structure of the mineral can alter the SiO_4 tetrahedra structure, resulting in intraparticle diffusion. From the speciation of Ni, above pH 8 the main species present in solution are $Ni(OH)_2$ and $Ni(OH)_3^-$ (**Figure 1** and **Figure 2**). These species will not favour the sorption by electrostatic interaction because of the neutrality of $[Ni(OH)_2]$ and negative charge of $Ni(OH)_3^-$. The neutrality and charge of $Ni(OH)_2$ and $Ni(OH)_3^-$ do not affect intraparticle diffusion, which has not been accounted for in this work. Despite the electronic neutrality and negative charge on some of the Ni species, sorption can occur though other mechanisms such as ligand exchange with partially deprotonated silanol groups (Schindler et al., 1976; Stumm, 1995). Another reason can be due to the non-attainment of equilibrium or steady state in the experimental.

Modelling the experimental data required the adjustment of input parameters, such as the mineral composition, the Log K values for the metal-solid complex formation taking into consideration the fact that two types of complexes may be formed (monodentate and bidentate) and the particle radius. Thus, the complexation constants are obtained from fitting the JChess data to the experimental model. For the simple case (NaCl free solution), the following input parameters were used; exchange capacity 5×10^{-2} μmol·m^{-2} calculated from titrimetric experiments with 0.1 g of Rose Quartz (particle size of 46 to 250 microns) and Log K values of −5 for both monodentate (Quartz-O-Ni$^+$) and bidentate (Quartz-O)2Ni. Based on the calculation from JChess, the output console showed the concentration of Ni to be 1.8×10^{-11} and 4.9×10^{-22} mol·dm^{-3} for monodentate and bidentate binding respectively. The implication is that at the determined Log K values for monodentate and bidentate formation, the sorption of Ni to quartz is overwhelmingly monodentate.

The effect of NaCl on the complexation of Ni to quartz is summarised (for NaCl free, 0.05 and 0.1 mol·dm^{-3} NaCl) in terms of the number of Ni bonded sites present in the system, as shown in **Table 5**, using the same Log K value of −7 for mono and bidentate formations, as was used for Ni sorption to quartz in NaCl

free system.

$$\equiv \text{Quartz} - \text{OH} + \text{Ni}^{2+} \rightleftharpoons \equiv \text{Quartz} - \text{ONi}^{+} \quad \text{LogK} = -7$$

$$\equiv \text{Quartz} - \text{OH} + \text{Ni}^{2+} \rightleftharpoons \left(\equiv \text{Quartz} - \text{O}\right)_2 \text{Ni} \quad \text{LogK} = -7$$

From Table 5 the most probable sorption mechanism can be determined based on the concentration of the sites. From the table, a monodentate complexation with Ni is the most likely to form in solution. The table also shows the effect of Na^+ on the available sorption sites. Comparing modelled data for the three systems, results show that the maximum amount bound was in the order: 9.4×10^{-6} mol·g^{-1} (NaCl free) > 6.5×10^{-6} (0.05 mol·dm^{-3} NaCl) > 3.2×10^{-6} (0.1 mol·dm^{-3} NaCl), all values at the pH of maximum sorption. Thus, it can be concluded that the presence of NaCl in solution affected the sorption capacity of quartz.

3.6. Ni Sorption to Orthoclase Feldspar

Feldspars are anhydrous three-dimensional aluminosilicates of linked SiO_4 and AlO_4 tetrahedra that contain cavities that can hold mono and divalent cations to maintain electrical neutrality (Sparks, 2002). They can be divided into two main groups; alkali feldspars ranging from K aluminosilicates (Orthoclase Feldspars) and Na to Ca aluminosilicates (Plagioclase Feldspars). Feldspar minerals are thermodynamically unstable in the near-surface environment and their surfaces are well known to react readily with aqueous solutions, leading to incongruent dissolution at low pH values, but congruent dissolution at neutral and high pH values (Chardon et al., 2008). Orthoclase Feldspar (OF) is chosen as a representative sample of feldspar. Orthoclase is a common constituent of most granitic rocks. Typically, the pure potassium end-member of orthoclase forms a solid solution with albite, (plagioclase feldspar mineral).

Results obtained from varying pH experiments in three different NaCl environments are shown in the isotherms Figure 8. From the results regions of significant rise in sorption are observed for the three systems, from which proton stoichiometry are defined as shown in Table 4. Between pH of 3.5 and 7.5, sorption showed a gentle increase, governed by cation exchange process. However, sorption showed a significant increase between pH 7.5 to 9.5 as shown in Figure 10. The effect of NaCl is not clearly seen. The fact that Ni sorption to feldspar showed similar pattern in the three systems studied (Figure 10) is supported by modelled data presented in Table 6. Sorption parameters are shown in Table 4.

Granitic rocks mineral particles can be represented as a semi-infinite homogeneous porous solid which bears a permanent negative charge uniformly distributed, resulting from isomorphic substitution in the structure (Kraepiel, 1999). Thus, granitic minerals such as feldspars may sorb radionuclides in a large pH range, as seen in Figure 10. Sorption spans a large pH range with no clearly defined region of steep rise in sorption, indicating that sorption can be dominated by cation exchange mechanism and surface complexation, involving both weak and strong sites (The "strong sites," have a high affinity for metals,

and are responsible for adsorption at low metal concentrations, and the "weak sites," play a role only at high pH or high metal concentrations, when the strong sites are saturated (Kraepiel, 1999). The proton stoichiometry was calculated in the range 0.5 to 1 highlighting low deprotonation involved in the system. The proton stoichiometry relates to the number of protons released in the solid-metal complexation process. Highly deprotonating systems will have proton stoichiometry > 1, as such the metal-solid complex formation will be controlled by the pH of the system. Thus, from the results obtained for Ni sorption to feldspar, it can be concluded that no single mechanism (CEC and SCM) is solely applicable to the sorption results obtained.

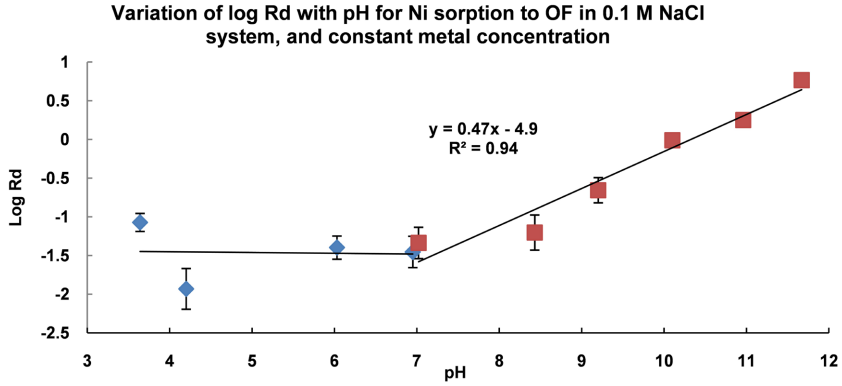

Figure 10. Log Rd variation with pH for Ni sorption to Orthoclase Feldspar. Figure relates to **Figure 10** (0.1 mol·dm^{-3} NaCl system). Figure shows region of significant rise in sorption with pH, with the slope defining the proton stoichiometry (<1) and the deprotonation constant as the intercept.

Table 6. Concentration of site occupancy for Ni sorption to feldspar in different NaCl environments. Log K values of 0.1 and −0.5 were used for mono and bidentate systems respectively. Exchange capacity 3.1 × 10^{-2} μmol·m^2 calculated from titrimetric experiments with 0.1 gram of feldspar (particle size of 46 - 250 microns). Table shows no major difference between the three systems and sorption is dominated by the formation of monodentate complexes. The absence of Na-Solid complex formation indicates Na^+ is passive in the systems thus, no effect on the sorption profile.

Site	NaCl free (mol·dm^{-3})	0.05 mol·dm^{-3} NaCl (mol·dm^{-3})	0.1 mol·dm^{-3} NaCl (mol·dm^{-3})
≡Feldspar-O-Na	-	-	-
≡Feldspar-O-Ni^+	4.6×10^{-8}	4.7×10^{-8}	4.6×10^{-8}
(≡Feldspar-O)$_2$Ni	1.0×10^{-16}	5.9×10^{-18}	5.2×10^{-18}

3.7. Results from Surface Complexation Modelling-Feldspar

Surface complexation modelling was performed with feldspar in the presence of 0.1 mol·dm^{-3} Na^+ ions. The proton exchange capacity for OF was calculated as 3.1 × 10^{-2} μmol·m^{-2} from titration 0.1 g of feldspar with 2 M NaOH and particle radius of 2.7 nm. Running the program with stated output parameters, the concentration

of fixed Ni was calculated at different pH values. Setting Log K values at −1 and −1.5 for monodentate and bidentate respectively, the data obtained were compared with the experimental data as shown in Figure 11. The JChess isotherm was the best fit for the stated condition.

$$\equiv \text{Feldspar} - \text{OH} + \text{Ni}^{2+} \rightleftharpoons \equiv \text{Feldspar} - \text{ONi}^{+} \quad \text{LogK} = -1.0$$

$$\equiv \text{Feldspar} - \text{OH} + \text{Ni}^{2+} \rightleftharpoons (\equiv \text{Feldspar} - \text{O})_2\,\text{Ni} \quad \text{LogK} = -1.5$$

Figure 11 shows the sorption profile for Ni^{2+} in 0.05 mol·dm^{-3} NaCl. The results from the JChess model and the experimental data did not show any major differences. The conclusion is that there was a region of steep rise in sorption, and sorption increased gently with pH.

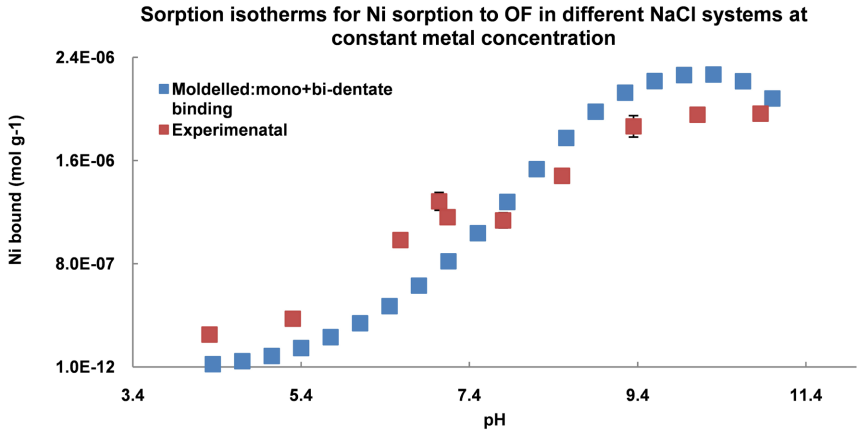

Figure 11. Varying pH sorption isotherms for Ni sorption to Orthoclase Feldspar. Figure showing data from experimental data and modelled, using the same experimental conditions, modelling done assuming mono and bidentate complex formation. Equilibrating ca. 8 days with liquid solid ratio of 200:1, at rtp.

From Figure 11, it can be concluded that the modelled data fitted the experimental data and sorption could be described thermodynamically using the assigned Log K values of −1 and −1.5 for mono and bidentate binding respectively, for Ni sorption in 0.05 mol·dm^{-3} NaCl systems.

JChess was used to model the effect of NaCl in the system, by running the program for NaCl free, 0.05 mol·dm^{-3} NaCl systems and 0.1 mol·dm^{-3} NaCl systems. Experimental results obtained for Ni^{2+} sorption to feldspar in the three systems (Figure 8) showed that the sorption profiles for the three systems did not vary, despite the presence of different amounts of NaCl in solution. Thus, this section aims to model sorption in the three systems and to observe the effect of NaCl using the concentration of sorption sites (Ni-Solid and Na-Solid) for the three systems. The concentration of sorption sites present is directly related to the sorption capacity.

Comparing the three systems (NaCl free, 0.05 and 0.1 mol·dm^{-3} NaCl) based on output report from JChess; results showed that Na^{+} did not affect the sorption in

all three systems. No complexation of Na^+ with the surface was observed at the stated conditions. The results agree with observation from the experimental data (Figure 10, no major difference is observed in the sorption profile for all three systems).

From Table 6 above the following conclusions can be drawn;

1) NaCl did not affect the sorption of Ni, in all three systems. This has been shown experimentally (see Figure 8) and by surface complexation modelling.

2) The most probable complexation mode is by Si-O-Ni complex (i.e. monodentate binding.

3.8. Ni Sorption to Muscovite Mica

Varying pH sorption experiments for Mica as in Figure 12 were performed in similar manner as those of quartz and feldspar. Analysing the data within the pH range studied showed that the sorption capacity did not vary. The sorption capacity (2×10^{-3} mol·g^{-1}) did not vary from low to high pH. Layered silicates contain two types of surface adsorption sites: those with a permanent charge, formed because of isomorphic substitution in the crystal structure, and with a pH-dependent charge appearing because of protonation or deprotonation of hydroxyl groups on the basal or edge surfaces of the tetrahedral or octahedral layers. Ion exchange reactions usually take place on the basal surface, where sites with an unbalanced structural charge are located. For mica, this charge is negative, and the sorption of cations on these sites only slightly depends on the pH value of the solution (Maslova et al., 2004). One other reason for the constancy in the sorption capacity from low to high pH can be due to the position on the point of zero charge (pH at which the net surface charge is zero) on the pH scale. With PZC for silicate minerals reported to be close to 2, and 4 to 6 for alumina minerals (Mahě et al., 2008), it is expected that PZC for mica will be <4. At PZC < 4 the surfaces will be negatively charged when present in a pH environment > 4, resulting in constancy in the sorption capacity.

In varying pH systems, adsorption sites are concentrated at edges ending with aluminol or silanol groups, which can accept or donate a hydrogen ion causing the appearance of an unbalanced surface charge. In contrast to ion exchange, surface complexation is determined by the pH value of the medium (Maslova et al., 2004). Maslova et al. (2004) studying the surface properties of cleaved mica, showed that only 5 to 10% of the total charge at pH 7 is due to pH-dependent adsorption sites. Hence, the ion exchange can take place at higher pH values. Thus, the following conclusions can be made:

1) Ni sorption is not affected by pH.

2) Ni sorption is not affected by the presence of NaCl.

3) Sorption is not affected by competition with Na ions.

4) Cation exchange represents the major sorption mechanism.

The high sorption capacity at low pH can be attributed to the mica structure; cations found in the interlayer hold the sheets together. In solutions, there is dis-

solution of the cations holding the layers together, resulting in excess permanent changes on the mica surfaces (Hans-Jurgen et al., 2004). This excess permanent negative charge is responsible for the high sorption capacity at low pH.

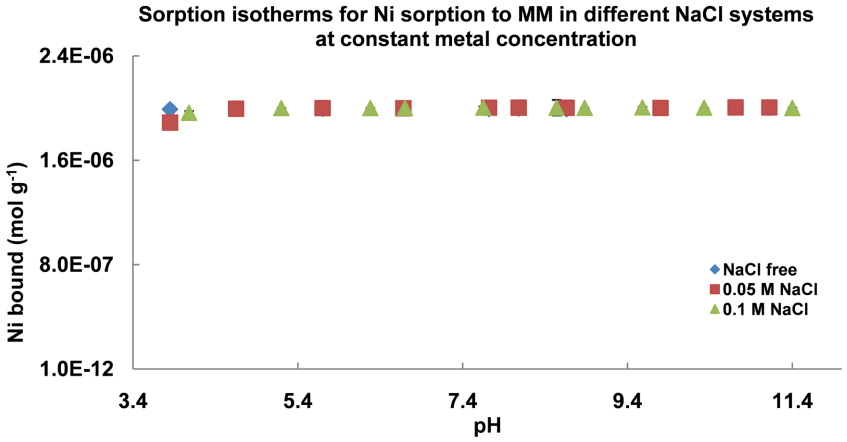

Figure 12. Varying pH sorption of Ni to Muscovite Mica at constant metal concentration of Ni. Figure showing sorption profile of Ni in different ionic strength environments, equilibrating ca. 8 days with liquid solid ratio of 200:1, at rtp.

Results from surface complexation modelling-Mica

The presence of permanent negative charge on the mica surface will cause surface complexation with metal ions. JChess geochemical code was used to model the sorption of Ni to Muscovite Mica (composition provided by JChess data base) as a representative sample of mica. The proton exchange capacity for Muscovite Mica (MM) was calculated as 70.4 μmol·m^{-2} from titration of 0.1 g of MM with 1 M NaOH and particle radius of 2.8 nm. Running the program with stated output parameters, the concentration of fixed Ni was calculated at different pH values. Setting Log K value at Log K = 5 for mono and bidentate. The data obtained were compared with the experimental data as shown in Figure 12.

$$\equiv \text{Muscovite} - \text{OH} + \text{Ni}^{2+} \rightleftharpoons \equiv \text{Muscovite} - \text{ONi}^{+} \quad \text{LogK} = 5$$

$$\equiv \text{Muscovite} - \text{OH} + \text{Ni}^{2+} \rightleftharpoons (\equiv \text{Muscovite} - \text{O})_2\,\text{Ni} \quad \text{LogK} = 5$$

Results showed no major difference between the experimental and the model. The following conclusions can be made:

1) Sorption takes place from low to high pH, for both predicted and experimental models.

2) The same sorption capacity is attained for both modelled and experimental data.

Running the JChess program in the presence of different concentrations of NaCl produced the data shown in Table 7.

The results shown in Table 7 indicated that NaCl did not influence the sorption based on the total number of sorption sites. These results confirm experimental findings that showed NaCl had no effect on the sorption of Ni to mica.

Table 7. Concentration of site occupancy Ni sorption to Muscovite Mica in different NaCl environments. Exchange capacity 3.1×10^{-2} μmol·m^2 calculated from titrimetric experiments with 0.1 gram of MM (particle size of 46 - 250 microns). Table shows no significant difference between the three systems and sorption is dominated by the formation of monodentate complexes.

Site	NaCl free (mol·dm^{-3})	0.05 mol dm^{-3} NaCl (mol·dm^{-3})	0.1 mol dm^{-3} NaCl (mol·dm^{-3})
≡muscovite-O-Na	-	-	-
≡muscovite-O-Ni$^+$	9.9×10^{-6}	1.0×10^{-5}	1.0×10^{-5}
(≡muscovite)$_2$Ni	2.2×10^{-15}	4.4×10^{-17}	2.2×10^{-17}

4. Conclusion

The following conclusions can be made after studying varying pH sorption profiles of selected granitic rocks and minerals in different NaCl concentrations, using different models.

1) Ni sorption is suppressed in the presence of NaCl, due to competition for the sorption sites;

2) Surface complexation constants for experimental data have been determined by fitting modelled data to experimental data.

Conflicts of Interest

The authors declare no conflicts of interest regarding the publication of this paper.

References

Allard, B., Beall, G. W., & Krajewski, T. (1980). The Sorption of Actinides in Igneous Rocks. *Nuclear Technology, 49,* 474-480. https://doi.org/10.13182/nt80-a17695

Allison, S. (2004). *Investigating Inorganic Colloids in the Near Field of a Waste Repository*. Doctoral Thesis, Loughborough University, Department of Chemistry (Radiochemistry group).

Anderson, E. B., Rogozin, Y. M., Smirnova, E. A., Bryzgalova, R. V., Andreeva, N. R., Malimonova, S. I. et al. (2007). Sorption-Barrier Properties of Granitoids and Andesite-Basaltic Metavolcanites with Respect to Am(III) and Pu(IV): 1. Absorption of Am and Pu from Groundwater on Monolithic Samples of Granitoids and Andesite-Basaltic Metavolcanites. *Radiochemistry, 49,* 305-312. https://doi.org/10.1134/s1066362207030186

Andersson, J. (2008). *Introduction of the Safety Case*. Presentation at the Third FUNMIG Training Course, Barcelona.

Andersson, K. (1988). *SKI Project 90: Chemical Data*. Swedish Nuclear Power Inspectorate Report, SKI-TR-91-21.

Argonne National Laboratory EVS (2005). *Human Health Fact Sheet, August 2005*.

Australian Government (2023). *Department of the Environment and Water Resources 2007-09-27*.

Baston, G. M. N., Berry, J. A., Bond, K. A., Boult, K. A., Brownsword, M., & Linklater, C. M. (1994). Effects of Cellulosic Degradation Products on Uranium Sorption in the Geosphere. *Journal of Alloys and Compounds, 213,* 475-480. https://doi.org/10.1016/0925-8388(94)90965-2

Bernard, N. (1995). *Adsorption of Radionuclides on Minerals. Studies Illustrating the Effect of Solid Phase Selectivity and of Mechanisms Controlling Sorption Processes*. Oak Ridge Institute for Science and Education.

Bradbury, M. H., & Baeyens, B. (2009). Sorption Modelling on Illite Part I: Titration Measurements and the Sorption of Ni, Co, Eu and Sn. *Geochimica et Cosmochimica Acta, 73,* 990-1003. https://doi.org/10.1016/j.gca.2008.11.017

Chardon, E. S., Bosbach, D., Bryan, N. D., Lyon, I. C., Marquardt, C., Römer, J. et al. (2008). Reactions of the Feldspar Surface with Metal Ions: Sorption of Pb(II), U(VI) and Np(V), and Surface Analytical Studies of Reaction with Pb(II) and U(VI). *Geochimica et Cosmochimica Acta, 72,* 288-297. https://doi.org/10.1016/j.gca.2007.10.026

Cresser, M., Killham, K., & Edwards, T. (1993). *Soil Chemistry and Its Applications*. Cambridge University Press. https://doi.org/10.1017/cbo9780511622939

Dähn, R., Scheidegger, A. M., Manceau, A., Schlegel, M. L., Baeyens, B., Bradbury, M. H. et al. (2003). Structural Evidence for the Sorption of Ni(II) Atoms on the Edges of Montmorillonite Clay Minerals: A Polarized X-Ray Absorption Fine Structure Study. *Geochimica et Cosmochimica Acta, 67,* 1-15. https://doi.org/10.1016/s0016-7037(02)01005-0

Ebong, F. S., & Nick, E. (2008). Modelling the Sorption of Nickel to Granite and Its Constituent Minerals. In *NRC7-Seventh International Conference on Nuclear and Radiochemistry Budapest Hungary* (pp. 134-138).

Ebong, F. S., & Nick, E. (2012). Modelling the Sorption of 63Ni to Granitic Materials: Application of the Component Additive Model. *Journal of Environmental Science and Engineering B, 1,* 281-292.

Ebong, F.S., & Nick, E. (2011). Sorption of Ni and Eu in a Multi-Element System. *Journal of Materials Science and Engineering B, 1,* 504-515. https://doi.org/10.17265/2161-6221/2011.09.015

Everett, A. J. (1998). *Adsorption of Metals by Geomedia-Data Analysis Modelling Controlling Factors and Related Issues*. Battelle, Pacific Northwest Laboratory.

Goldberg, S., Criscenti, L. J., Turner, D. R., Davis, J. A., & Cantrell, K. J. (2007). Adsorption-Desorption Processes in Subsurface Reactive Transport Modeling. *Vadose Zone Journal, 6,* 407-435. https://doi.org/10.2136/vzj2006.0085

Guillaumont, R. (1994). Radiochemical Approaches to the Migration of Elements from a Radwaste Repository. *Radiochimica Acta, 66,* 231-242. https://doi.org/10.1524/ract.1994.6667.s1.231

Guo, Z., Li, Y., & Wu, W. (2010). Sorption of U(VI) on Goethite: Effects of Ph, Ionic Strength, Phosphate, Carbonate and Fulvic Acid. *Applied Radiation and Isotopes, 67,* 996-1000. https://doi.org/10.1016/j.apradiso.2009.02.001

Hans-Jurgen, B., Graf, K., & Kappl, M. (2004). *Physics and Chemistry of Interfaces*. Wiley Inter-Science.

Hayes, K. F., & Katz, L. E. (1996). Application of X-Ray Absorption Spectroscopy for Surface Complexation Modeling of Metal Ion Sorption. In P. V. Brady (Ed.), *Physics and Chemistry of Mineral Surfaces* (pp. 147-223). CRC Press. https://doi.org/10.1201/9781003068945-3

Hering, J. G., & Kraemer, S. (1994). Kinetics of Complexation Reactions at Surfaces and in Solution: Implications for Enhanced Radionuclide Migration. *Radiochimica Acta, 66,* 63-72. https://doi.org/10.1524/ract.1994.6667.special-issue.63

Higgo, J. J. W. (2007). *Review of Sorption Data Application Applicable to the Geological Environments of Interest for the Deep Disposal of ILW and LLW in the UK*. Nirex.

Hölttä, P., Siitari-Kauppi, M., Lindberg, A., & Hautojärvi, A. (1998). Na, Ca and Sr Retardation on Crushed Crystalline Rock. *Radiochimica Acta, 82,* 279-286. http://www.mindat.org https://doi.org/10.1524/ract.1998.82.special-issue.279

Jedináková-Křižová, V. (1998). Migration of Radionuclides in the Enviroment. *Journal of Radioanalytical and Nuclear Chemistry, 229,* 13-18. https://doi.org/10.1007/bf02389439

Kanungo, S. B. (1994). Adsorption of Cations on Hydrous Oxides of Iron: II. Adsorption of Mn, Co, Ni, and Zn onto Amorphous FeOOH from Simple Electrolyte Solutions as Well as from a Complex Electrolyte Solution Resembling Seawater in Major Ion Content. *Journal of Colloid and Interface Science, 162,* 93-102. https://doi.org/10.1006/jcis.1994.1013

Knol, R. J. J., de Bruin, K., de Jong, J., van Eck-Smit, B. L. F., & Booij, J. (2008). *In vitro* and *ex vivo* Storage Phosphor Imaging of Short-Living Radioisotopes. *Journal of Neuroscience Methods, 168,* 341-357. https://doi.org/10.1016/j.jneumeth.2007.10.028

Kraepiel, A. M. L., Keller, K., & Morel, F. M. M. (1999). A Model for Metal Adsorption on Montmorillonite. *Journal of Colloid and Interface Science, 210,* 43-54. https://doi.org/10.1006/jcis.1998.5947

L'Annunziata, M. F. (2004). *Handbook of Radioactivity Analysis* (2nd Ed.). Academic Press. https://doi.org/10.1016/B978-0-12-436603-9.X5000-5

Lützenkirchen, J., & Behra, P. (1996). On the Surface Precipitation Model for Cation Sorption at the (Hydr)Oxide Water Interface. *Aquatic Geochemistry, 1,* 375-397. https://doi.org/10.1007/bf00702740

Mahé, M., Heintz, J., Rödel, J., & Reynders, P. (2008). Cracking of Titania Nanocrystalline Coatings. *Journal of the European Ceramic Society, 28,* 2003-2010. https://doi.org/10.1016/j.jeurceramsoc.2008.02.002

Maslova, M. V., Gerasimova, L. G., & Forsling, W. (2004). Surface Properties of Cleaved Mica. *Colloid Journal, 66,* 322-328. https://doi.org/10.1023/b:coll.0000030843.30563.c9

McKinley, I. G., & Hadermann, J. (1984). *Radionuclide Sorption Data Base for Swiss Safety Assessment*. Nagra Technical Report NTB-84-40, Nagra, Baden Switzerland.

Mellado, J., Tarancón, A., García, J. F., Rauret, G., & Warwick, P. (2005). Combination of Chemical Separation and Data Treatment for ^{55}Fe, ^{63}Ni, ^{99}Tc, ^{137}Cs and ^{90}Sr/^{90}Y Activity Determination in Radioactive Waste by Liquid Scintillation. *Applied Radiation and Isotopes, 63,* 207-215. https://doi.org/10.1016/j.apradiso.2005.03.003

Muuronen, S., Kämäräinen, E., Jaakkola, T., Pinnioja, S., & Lindberg, A. (1985). Sorption and Diffusion of Radionuclides in Rock Matrix and Natural Fracture Surfaces Studied by Autoradiography. *MRS Proceedings, 50,* 747-754. https://doi.org/10.1557/proc-50-747

Ohnuki, T. (1994). Sorption Characteristics of Strontium on Sandy Soils and Their Components. *Radiochimica Acta, 64,* 237-246. https://doi.org/10.1524/ract.1994.64.34.237

Papelis, C. (2001). Cation and Anion Sorption on Granite from the Project Shoal Test Area, near Fallon, Nevada, USA. *Advances in Environmental Research, 5,* 151-166. https://doi.org/10.1016/s1093-0191(00)00053-8

Rumynin, V. G., Konosavsky, P. K., & Hoehn, E. (2005). Experimental and Modeling Study of Adsorption-Desorption Processes with Application to a Deep-Well Injection Radioactive Waste Disposal Site. *Journal of Contaminant Hydrology, 76,* 19-46. https://doi.org/10.1016/j.jconhyd.2004.07.008

Sarah, S. (1994). *First Year PhD Report* (p. 87). Environmental Radiochemistry Group, Department of Chemistry, Loughborough University.

Scheidegger, A. M., Sparks, D. L., & Fendorf, M. (1996). Mechanisms of Nickel Sorption on Pyrophyllite: Macroscopic and Microscopic Approaches. *Soil Science Society of America Journal, 60,* 1763-1772. https://doi.org/10.2136/sssaj1996.03615995006000060022x

Scheuerer, C., Schupfner, R., & Schüttelkopf, H. (1995). A Very Sensitive LSC Procedure to Determine Ni-63 in Environmental Samples, Steel and Concrete. *Journal of Radioanalytical and Nuclear Chemistry Articles, 193,* 127-131. https://doi.org/10.1007/bf02041926

Schindler, P. W., Fürst, B., Dick, R., & Wolf, P. U. (1976). Ligand Properties of Surface Silanol Groups. I. Surface Complex Formation with Fe^{3+}, Cu^{2+}, Cd^{2+}, and Pb^{2+}. *Journal of Colloid and Interface Science, 55,* 469-475. https://doi.org/10.1016/0021-9797(76)90057-6

Sparks, D. L. (2002). *Environmental Soil Chemistry* (2nd Ed.). University of Delaware.

Sposito, G. (1984). *The Surface Chemistry of Soils*. Oxford University Press.

Stumm, W. (1995). The Inner-Sphere Surface Complex: A Key to Understanding Surface Reactivity. *Advances in Chemistry, 244,* 1-32. https://doi.org/10.1021/ba-1995-0244.ch001

Ticknor, K. V. (1994). Sorption of Nickel on Geological Materials. *Radiochimica Acta, 66,* 341-348. https://doi.org/10.1524/ract.1994.6667.s1.341

Treado, P. A., & Chagnon, P. R. (1961). Neutron Capture Gamma-Ray Spectra of the Nickel Isotopes. *Physical Review, 121,* 1734-1739. https://doi.org/10.1103/physrev.121.1734

Tripathy, S. S., Bersillon, J., & Gopal, K. (2006). Adsorption of Cd^{2+} on Hydrous Manganese Dioxide from Aqueous Solutions. *Desalination, 194,* 11-21. https://doi.org/10.1016/j.desal.2005.10.023

United States Environmental Protection Agency (USEPA) (1999) *The Kd Model, Measurement Methods, and Application of Chemical Reaction Codes Volume 1*.

van der Lee, J. (2003). *JCHESS Version 2 Release 3*. Centre de Géosciences École Nationale Supérieure des Mines de Paris.

Vandergraaf, T. T., Drew, D. J., Archambault, D., & Ticknor, K. V. (1997). Transport of Radionuclides in Natural Fractures: Some Aspects of Laboratory Migration Experiments. *Journal of Contaminant Hydrology, 26,* 83-95. https://doi.org/10.1016/s0169-7722(96)00060-5

Yoshida, T., & Suzuki, M. (2006). Migration of Strontium and Europium in Quartz Sand Column in the Presence of Humic Acid: Effect of Ionic Strength. *Journal of Radioanalytical and Nuclear Chemistry, 270,* 363-368. https://doi.org/10.1007/s10967-006-0358-4